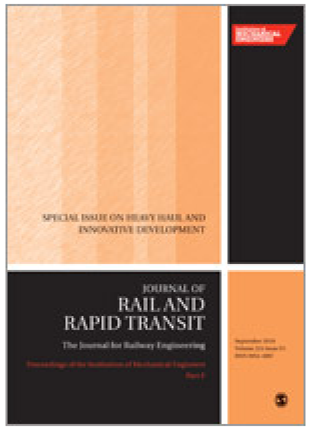

Numerical investigation on loading pattern of railway concrete slabs

Journal:	*Part F: Journal of Rail and Rapid Transit*
Manuscript ID	JRRT-24-0046.R1
Manuscript Type:	Article
Date Submitted by the Author:	25-Jun-2024
Complete List of Authors:	Liravi, Hassan; Universitat Politecnica de Catalunya Khajehdezfuly, Amin; Shahid Chamran University of Ahvaz, Department of Civil Engineering, Faculty of Engineering Sadeghi, Javad; Iran University of Science and Technology, Railway Eng. Aela, Peyman; The Hong Kong Polytechnic University, Civil and Environmental Engineering Shafieyoon, Yazdan; Universitat Politecnica de Catalunya A. Shiraz, Amir; Universitat Politecnica de Catalunya
Keywords:	Concrete slab track design, Field test, 2D finite element model, Loading pattern, Railway
Abstract:	Despite the recent surge in the construction of ballast-less railway tracks, there exists a notable research gap concerning the rail seat load (RSL) associated with these track types. The RSL is the load transferred from the rail to the fastening system, the plate beneath the rail and the rail pad. The prediction of RSL in ballasted track systems is widely investigated, however, there has been a relative lack of research into the ballast-less railway track systems. In this paper, a 2D finite element model (2D FEM) was adopted to evaluate the RSL concerning the effective parameters, including sleeper spacing, track stiffness and the flexural modulus of the rail. The numerical model was validated through a field test performed in the study. Moreover, a mathematical expression was proposed to determine the RSL ratio for concrete slab tracks. The RSL directly correlates with the sleeper spacing and the fastening stiffness, while this relation with the flexural rigidity is inverse. Based on the results, it was found that the RSL ratio obtained from the conventional methods differed considerably from the proposed mathematical expression. More specifically, this difference was observed

	in almost all of the values in the sleeper spacing and flexural rigidity of rail for the Kerr model except 0.68 m and 5 MN.m2, respectively.

Note: The following files were submitted by the author for peer review, but cannot be converted to PDF. You must view these files (e.g. movies) online.
rejrrt240046_r1urgentfinalfilesrequired.zip

Journal Title
XX(X):1–10
©The Author(s) 2016
Reprints and permission:
sagepub.co.uk/journalsPermissions.nav
DOI: 10.1177/ToBeAssigned
www.sagepub.com/
SAGE

Numerical investigation on loading pattern of railway concrete slabs

Hassan Liravi[1], Amin Khajehdezfuly[2], Javad Sadeghi[3], Peyman Aela[4], Yazdan Shafieyoon[1] and Amir A. Shiraz[1]

Abstract

Despite the recent surge in the construction of ballastless railway tracks, there exists a notable research gap concerning the rail seat load (RSL) associated with these track types. The RSL is the load transferred from the rail to the fastening system, the plate beneath the rail and the rail pad. The prediction of RSL in ballasted track systems is widely investigated, however, there has been a relative lack of research into the ballastless railway track systems. In this paper, a 2D finite element model (2D FEM) was adopted to evaluate the RSL concerning the effective parameters, including sleeper spacing, fastening system stiffness and the flexural modulus of the rail. The numerical model was validated through a field test performed in the study. Moreover, a mathematical expression was proposed to determine the RSL ratio for concrete slab tracks. The RSL directly correlates with the sleeper spacing and the fastening stiffness, while this relation with the flexural rigidity is inverse. Based on the results, it was found that the RSL ratio obtained from the conventional methods differed considerably from the proposed mathematical expression. More specifically, this difference was observed in almost all of the values in the sleeper spacing and flexural rigidity of rail for the Kerr model except 0.68 m and 5 $\mathrm{MN.m^2}$, respectively.

Keywords

Concrete slab track design, Field test, 2D finite element model, Loading pattern, Railway

Introduction

Ballastless railway track systems (often called slab tracks) have gained significant attention worldwide owing to their numerous advantages over conventional ballasted ones. These benefits may manifest differently, including increased safety, reduced life cycle costs, and enhanced performance[1]. In more specific terms, enhanced dynamic performance[2], better vehicle stability[3], and, perhaps most importantly, low maintenance requirements[4]. However, there has been a relative lack of research into the design and construction of ballastless track systems, particularly when compared with ballasted tracks. Railway track structural analysis involves understanding the load path as it passes through the vehicle's wheels onto the rail, sleepers, and down into the track substructure. Each fastening system, plate beneath the rail and rail pad carries a portion of the load, known as the rail seat load (RSL). For the design of railway track components, it is crucial to be able to compute RSL accurately[5]. Over the years, numerous studies have been conducted to predict and measure the RSL. In these studies, which mostly focused on ballasted tracks, experimental investigations, numerical methods, and analytical models were employed.

The calculation of the RSL experimentally, i.e., field investigations and laboratory experiments, has been widely considered on the ballasted tracks compared to other methods. A mathematical expression was developed for the RSL distribution pattern on the different types of sleepers[6,7]. For better measurement of the RSL distribution, several tests performed on the different loading scenarios as well as various fastening systems[8]. Wei et al. determined the RSL and load path in the field to aid in the recommendations for the mechanistic design of various components within the fastening system[9]. Utilizing strain gauges, it is possible to determine the amount of load transferred to the sleeper, and from this, the RSL value was calculated[10]. Wheeler et al. measured the rail strains and shear forces and combined them with the static wheel loads to compute the RSL[11]. Furthermore, considering the track substructure stiffness, Grasse determined the load distribution of three adjacent sleepers (i.e., ranging from 44-56 % of the vertical wheel load)[12]. Manda et al. identified how the characteristics of track components (e.g., stiffness, geometry, and interface) affect the flow of forces in the vertical direction and fastening systems[13]. Askarinezhad et al. performed research on the wheel-rail contact-impact force. The vertical impact force at rail joints through the

[1]Acoustical and Mechanical Engineering Laboratory (LEAM), Universitat Politècnica de Catalunya (UPC). c/ Colom, 11, 08222 Terrassa (Barcelona), Spain.
[2]Department of Civil Engineering, Faculty of Civil Engineering and Architecture, Shahid Chamran University of Ahvaz, Ahvaz 6135783151, Iran.
[3]School of Railway Engineering, Iran University of Science and Technology, Tehran, Iran.
[4]Department of Civil and Environmental Engineering, The Hong Kong Polytechnic University, Hung Hom, Kowloon, Hong Kong, China.

Corresponding author:
Hassan Liravi, Acoustical and Mechanical Engineering Laboratory (LEAM), Universitat Politècnica de Catalunya (UPC). c/ Colom, 11, 08222 Terrassa (Barcelona), Spain.
Email: hassan.liravi@upc.edu

strain-gauge instrumentation was measured[14]. Gao et al. conducted laboratory experiments and applied a 3D FEM modelling to analyse the load path through prestressed concrete sleepers and the vertical compression stress distribution beneath the rail seats[15]. Matrix-based tactile surface sensors (MBTSSs) instrumentation technology has been implemented to determine the load distribution over consecutive sleepers[16]. A series of tests were conducted by Greve et al. to better understand the distribution of RSL, its effects on rail seat deterioration, and the factors involved[17]. Zhang et al. carried out a field test on an operational track using the MBTSSs to investigate the characteristics of the dynamic rail pad force and its stress distribution[18].

Numerical methods aid in determining the RSL by analysing the dynamic behaviour of railway systems and predicting load distribution on the rail seat. A thorough comparison of the RSL expressions was provided by Van Dyk and his colleagues, evaluating the current practices on RSL calculation to develop existing concrete sleeper and fastening system design standards in the ballasted railway tracks[19]. Momoya et al. investigated the applied load on large-spacing concrete sleepers using FE analysis and validated their model by measuring RSLs at the site for the ballasted railway tracks[20]. Lojda et al. proposed a simplified method for calculating load distribution and rail deflections on ballasted railway tracks, incorporating sleeper stiffness. This method takes into account both the bending and shear stiffness of the sleeper and applies to both newly constructed and tamped tracks[21]. Shi et al. introduced a hybrid numerical model to investigate the mechanical characteristics of railway transition zones. The proposed model was validated through experimental methods, including the measurement of RSL[22].

The application of analytical models for determining the RSL has been relatively understudied in scholarly research. Trizotto et al. conducted research concerning the development of an analytical elastic model for the longitudinal response of rails and fasteners. Using their validated method, they quantified the distribution and magnitude of longitudinal RSLs[23].

As mentioned earlier, the prediction of RSL in ballasted track systems is widely investigated. Considering the remarkable development of railway slab tracks in urban railroads, a similar procedure to that used for ballasted railway tracks is required to analyse and design the railway slab tracks. Moreover, only a handful of studies have predicted RSL in slab track systems. The International Association of Public Transport (UITP) proposed the Zimmermann equation as an appropriate distribution factor for train loading on ballastless tracks. Since only one wheel is considered in this equation, the effects of the other wheels of railway vehicles are ignored, thereby decreasing the accuracy of the output[24]. There are, however, some overestimations of the loading pattern[2] so, more accurate loading patterns are required for slab tracks. Sadeghi et al. demonstrated how the load transfers from the rail to the support slabs by conducting comprehensive field and laboratory tests on concrete railway slab tracks. However, due to the nature of the experimental tests, there is a limitation in the effect of all influencing parameters on the RSL in railway slab track[25].

A review of the literature shows that previous studies have either been conducted solely for ballasted tracks[26,27] or have used limited parameters for numerical study[15] or employed the well-known recommendation of wheel load distribution over three adjacent sleepers which is an approximate prediction of RSL[28]. Also, due to the experimental nature of some of the proposed models, there was a limitation to the investigation of all influencing parameters on the RSL in railway slab tracks[25]. To address these drawbacks, a comprehensive assessment is required, and this research aims to fulfil this need. For this purpose, a numerical model was developed that examines the effect of sleeper spacing, fastening system stiffness and the flexural modulus of the rail on RSL. The numerical model was validated through a field test on a subway.

The paper is organised as follows: in section 2, the proposed 2D FEM, which was developed in the FORTRAN environment, is explained in detail. Section 3 is dedicated to the experimental validation of the developed numerical model. In section 4, a parametric study is conducted in order to gain a deeper understanding of the role of the effective parameters on the quantity of the RSL and the determination of the dominant effective variables. Afterwards, in section 5 an accurate mathematical expression was developed based on the results obtained from the parametric study. Lastly, in section 6, the proposed mathematical is compared with conventional approaches used in current practices.

Description of the model

In this study, a 2D FEM was developed and implemented in FORTRAN environment to evaluate RSL in ballastless tracks. The model, illustrated in Fig. 1, incorporates various components including rail, fastening system, concrete slab, polyurethane layer, concrete base, and subgrade. Furthermore, the wheels are denoted as P_i, applied on the rails. It is important to note that the concrete slab is treated as a discontinuous beam. Furthermore, it is assumed that the train has the symmetric load distribution between both rail. According to literature review, the comparison of 2D and 3D models shows that for evaluating loads in the absence of horizontal curves, 2D models have sufficient accuracy[29]. Thus, it becomes possible to reduce the computational cost associated with the model, enabling an evaluation of diverse parameters, performing sensitivity analyses, and formulating a more comprehensive mathematical expression for RSL in slab tracks by using 2D model. This model, which is a further development of the model initially presented by Sadeghi et al[25], can calculate each fastening system force and longitudinal distribution factor under a static wheel load. The dynamics of rail tracks, particularly during the passage of a train, are influenced by the forces and vibrations induced by moving trains, impacting the RSL. This effect can be considered by applying the dynamic wheel load factor in the quasi-static approach. While this factor does not affect the vehicle's load distribution on each sleeper (i.e., the RSL ratio), it does impact the axle load and the RSL value. This means the dynamic wheel load factor is multiplied by the RSL value. The input parameters of the model comprise geometric features and mechanical properties of the track components. To apply the geometric characteristic,

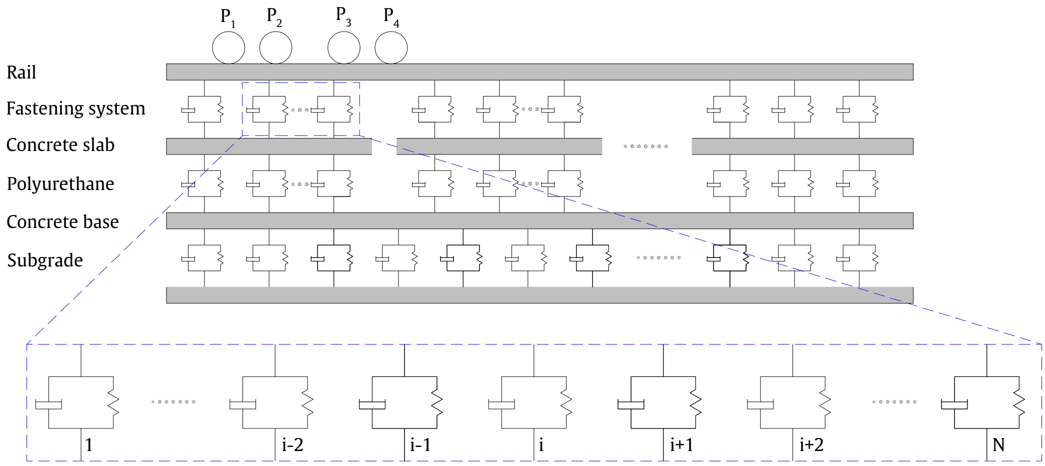

Figure 1. Longitudinal view of two-dimensional model including considered components.

various parameters were taken into account including the total number of fastening, the distance between the sleepers, the total number of fastening on each concrete slab, the distance between the first fastening from the edge of the slab and the boundary conditions of the rails, the slab and the concrete base. Moreover, in order to consider the mechanical characteristics of the track, flexural modulus of rail, slab and concrete base, fastening system stiffness, polyurethane layer stiffness and subgrade stiffness were considered in the model. Euler- Bernoulli beam theory[29–31] was used to model the rail, concrete slab and concrete base. Furthermore, fastening system, polyurethane layer and subgrade were simulated using discrete spring element[29,30]. The nonlinear mechanical properties of the fastening system can also influence the RSL ratio, particularly under dynamic conditions when a train is passing. However, in comparison to the linearized case, approximately 10% of the final results were affected by the nonlinear simulation of the vertical behaviour of the railway fastening system, within the investigated range of parameters[32]. Accordingly the linear behaviour was assumed for modeling the fastening system. The stiffness matrices associated with the Euler-Bernoulli beam and the spring are as follows:

$$\mathrm{K_b} = \frac{EI}{L^3}\begin{bmatrix} 12 & 6L & -12 & 6L \\ 6L & 4L^2 & -6L & 2L^2 \\ -12 & -6L & 12 & -6L \\ 6L & 2L^2 & -6L & 4L^2 \end{bmatrix} \quad (1)$$

$$\mathrm{K_s} = \begin{bmatrix} k & -k \\ -k & k \end{bmatrix} \quad (2)$$

In these matrices, $\mathrm{K_b}$ and $\mathrm{K_s}$ indicate the stiffness matrices of the beam and spring, respectively. Moreover, EI, L and k represent the flexural rigidity of the beam, length of the beam and stiffness of spring, respectively. The procedure of assembling matrices and vectors for different components was addressed in the literature[29], however, in this paper matrices of mass and damping were not taken into account. The static wheel load was applied to the centre of the model as a concentrated force. Consequently, the load was transferred to the underneath layers through the coupling system of the track. The stiffness matrix of the track was obtained according to the stiffness matrices of the rail, fastening system, concrete slab, polyurethane layer, concrete base and subgrade. Moreover, the external force vector of the track was calculated based on the wheel load position and shape functions of the beam element. These shape functions are presented in Eq. (3a) to Eq. (3d).

$$\mathrm{N_1} = \frac{1}{4}(1-\xi)^2(2+\xi) \quad (3a)$$

$$\mathrm{N_2} = \frac{1}{4}(1-\xi)^2(1+\xi) \quad (3b)$$

$$\mathrm{N_3} = \frac{1}{4}(1+\xi)^2(2-\xi) \quad (3c)$$

$$\mathrm{N_4} = \frac{1}{4}(1+\xi)^2(\xi-1) \quad (3d)$$

In the above equations, $\mathrm{N_i}$ and ξ indicate the shape functions and local coordinate system, respectively. Finally, to determine the RSL, the difference between the vertical deflection of the rail and the rail seat plate was derived and then multiplied by the stiffness of the rail pad, as detailed in the literature[25].

Validation of numerical results

In this section, the developed numerical model has been validated through an experimental field test conducted on a subway slab track. In the following sub-sections, firstly, the characteristics of the slab track on the field test, including both geometric and mechanical properties, as well as the test setup configuration, are comprehensively explained. Then, the results obtained from the field test are compared with those calculated by the numerical model.

Description of field test

The field test was performed at Kaveh metro station in Esfahan, one of the largest cities in Iran. The static test was conducted on a three-layer slab track (including concrete slab, rail and concrete base, respectively). Characteristics of the railway track in the field test are presented in Table 1. While the elasticity modulus of the concrete slab in the Esfahan metro was obtained in previous study[29], to ensure the accuracy of this value, Schmidt Hammer was also used in the field test. Six points (approximately, 8 m of the track)

Table 1. Characteristics of railway track in the field test[29]

Track layer	Considered parameters	Unit	Value
Rail	Flexural rigidity	Nm^2	3819900
Fastening system	Fastening space	m	0.6
	Rail pad stiffness	N/m	15×10^7
Concrete slab	Length	m	11.37
	Elasticity modulus	MPa	3.5×10^4
	Gap between slabs	m	0.0285
Polyurethane	Stiffness	N/m^3	11648000
Concrete base	Elasticity modulus	MPa	3.3×10^4
Subgrade	Stiffness	N/m^3	13.1×10^7

were considered for this test. The points were impacted ten times by the hammer. Consequently, the elasticity modulus of the concrete slab was obtained through the results and a good agreement was observed between the current values and those presented in the literature. The applicability and validity of the Schmidt Hammer have been investigated in the previous studies[33,34].

A two-axle shunter, type VTL200, with an axle load of 123.5 kN, a car length of 8.04 m, and a 4.5 m center-to-center axle distance in the bogie, was used for the loading procedure.

The stiffness of the rail pads was obtained in the previous work[25] where it was measured in the laboratory tests. Moreover, the subgrade stiffness was well documented in the reference[29]. Five sleepers were instrumented for data acquisition. A 1.8 m long section of rail was instrumented with a Linear Variable Differential Transformer (LVDT) and the absolute deflection of the slab in the centre line of fastenings was measured in five different points (Fig. 2). A test was conducted to obtain the vertical displacement of the slab. Additionally, the absolute vertical displacement was needed, which is why L-shaped steel bars were used. Therefore, L-shaped steels were provided and fixed on the benchmarks (Fig. 2). The LVDTs were perpendicularly applied on the slab and securely clamped to a steel rod which was attached to the rail web by a magnet support[29]. The absorption strength of the standard magnetic base (MB-B, Kanetec) is approximately 800 N which ensures enough strength for holding measuring instruments[25]. This range of absorption strength prevents any movement or sliding of the LVDT sensors. Moreover, LVDT 6 was used to measure the relative displacement between the rail and the slab.

Model validation and results comparison

Two sets of loading arrangements were chosen for the validation of the model. In the first loading scenario, the first wheel of the vehicle was located on the sixth sleeper and in the second case, the second wheel was on the twelfth sleeper. The absolute vertical displacements of the slab obtained from the models and the measurements are compared in Fig. 3. As indicated in this figure, slight discrepancies of up to 2% and 3% are observed between the predictions and the experimental values in the first and second load case scenarios, respectively. Since the RSL can be determined by multiplying the relative deflection between the rail and slab by the rail pad stiffness, the RSL was calculated and compared with experimental data obtained by LVDT 6. Fig. 3c shows the RSL amount in different location of second wheel. These slight differences confirm the accurate performance of the developed model.

Parametric study

In order to have a deep understanding of the influence of all effective parameters on the quantity of RSL and determination of the dominant effective parameters, a parametric study was conducted on different variables, including the flexural rigidity of the rail, sleeper spacing, fastening stiffness, flexural rigidity of the concrete slab, polyurethane stiffness, the flexural rigidity of the concrete base, and subgrade stiffness. The range of variation of each parameter and the variation steps for the parametric study are illustrated in Table 2. The maximum and minimum values of the parameters are also demonstrated in Table 2. In this paper, three types of rail profiles including UIC60, UIC54, and S49 are considered for examination. Once the upper and lower limits of the considered parameters were defined, the dominant parameters can be determined for further steps. For this purpose, firstly, a reference model with defined variables was considered. Then, all the variables were evaluated individually based on the initial values of the reference model. In this procedure, all parameters remain invariant based on the reference model except the target variable which changes in the defined limits shown in Table 2. Fig. 4 presents the results of the effect of different parameters on RSL. As can be observed in Fig. 4a, by increasing the sleeper spacing in the range of 0.5m to 0.75m, the RSL ratio rises smoothly. According to the literature[25], the flexural rigidity of the rail has an inverse relationship with the RSL ratio. However, due to the insignificant difference in the current rail type profiles, a small steepness can be seen in Fig. 4b. Moreover, according to Figs. 4e, 4f and 4g, the effects of polyurethane stiffness, the flexural rigidity of the concrete base layer, and subgrade stiffness are insignificant. Comparing these values of Fig. 4b with those of Fig. 4d confirms that the flexural rigidity of the rail is a more effective parameter than the flexural rigidity of the slab. Considering these results, fastening stiffness, the flexural rigidity of the rail and sleeper spacing were chosen as dominant effective parameters on RSL. Therefore, an extensive parametric study was performed to develop a mathematical expression for determining the RSL in the railway slab track.

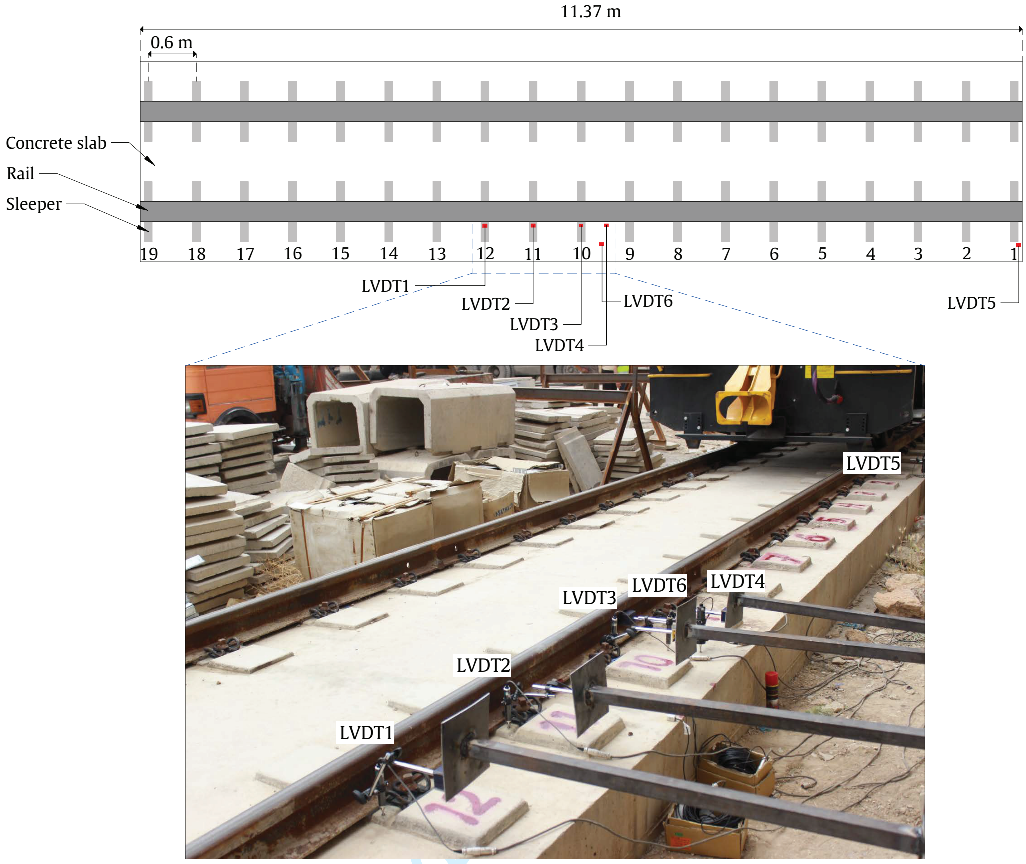

Figure 2. Top schematic view of field test setup.

Table 2. Ranges of variation of each parameter

Variable	Description	Step/type
Sleeper spacing [m]	From 0.5 to 0.75	0.05
Flexural rigidity of rail [$\mathrm{Nm^2}$]	3632000	S49
	4675800	UIC54
	6755700	UIC60
Fastening stiffness [MN/m]	From 60 to 600	90
Flexural rigidity of slab [$\mathrm{MNm^2}$]	From 90 to 300	30
Polyurethane stiffness [$\mathrm{MN/m^2}$]	From 100 to 1000	100
Flexural rigidity of concrete base[$\mathrm{MNm^2}$]	From 60to 150	10
Subgrade stiffness [$\mathrm{MN/m^2}$]	From 120 to 480	60

Development of the mathematical expression

According to the previous section, the sleeper spacing, the fastening stiffness, and the flexural rigidity of the rail were selected as the dominant effective parameters by analysing the effect of different parameters on RSL. To develop the mathematical expression with high regression value $R^2 \geq 0.8$, numerous parametric studies were executed. For this purpose, the correlation matrix was used to measure how strong the effects of these variables are on the RSL ratio. As indicated in Table 3, the correlation coefficient between each of the two different variables is zero, except for variables versus rail seat load ratio, which means influencing parameters are independent. The correlation coefficient of the RSL ratio with the sleeper spacing, the fastening stiffness and the flexural rigidity of the rail are 0.194, 0.867 and -0.091, respectively. The magnitude of the correlation coefficient quantifies the intensity of the relationship or association between two variables. The larger the absolute value of the correlation coefficient, the stronger the relationship between the variables. According to Table 3, the rail profile has the least correlation coefficient $R^2 = -0.091$ which means that it has an inconsiderable inverse influence on the RSL ratio. The most effective variable is the fastening stiffness which has a direct relationship with the RSL. As a result, the most accurate multivariable nonlinear mathematical expression was derived to determine the RSL ratio (denoted as $\mathrm{Q_r}$) using XLSTAT[35],

$$\mathrm{Q_r} = 1.17 \times 10^{-5} \frac{(L_s + 6.3)^5 \times \left(K_f + 2.1 \times 10^8\right)}{EI_r + 1.2 \times 10^8} \qquad (4)$$

where L_s, K_f and EI_r represent the sleep spacing (m), fastening system stiffness (N/m) and flexural rigidity of

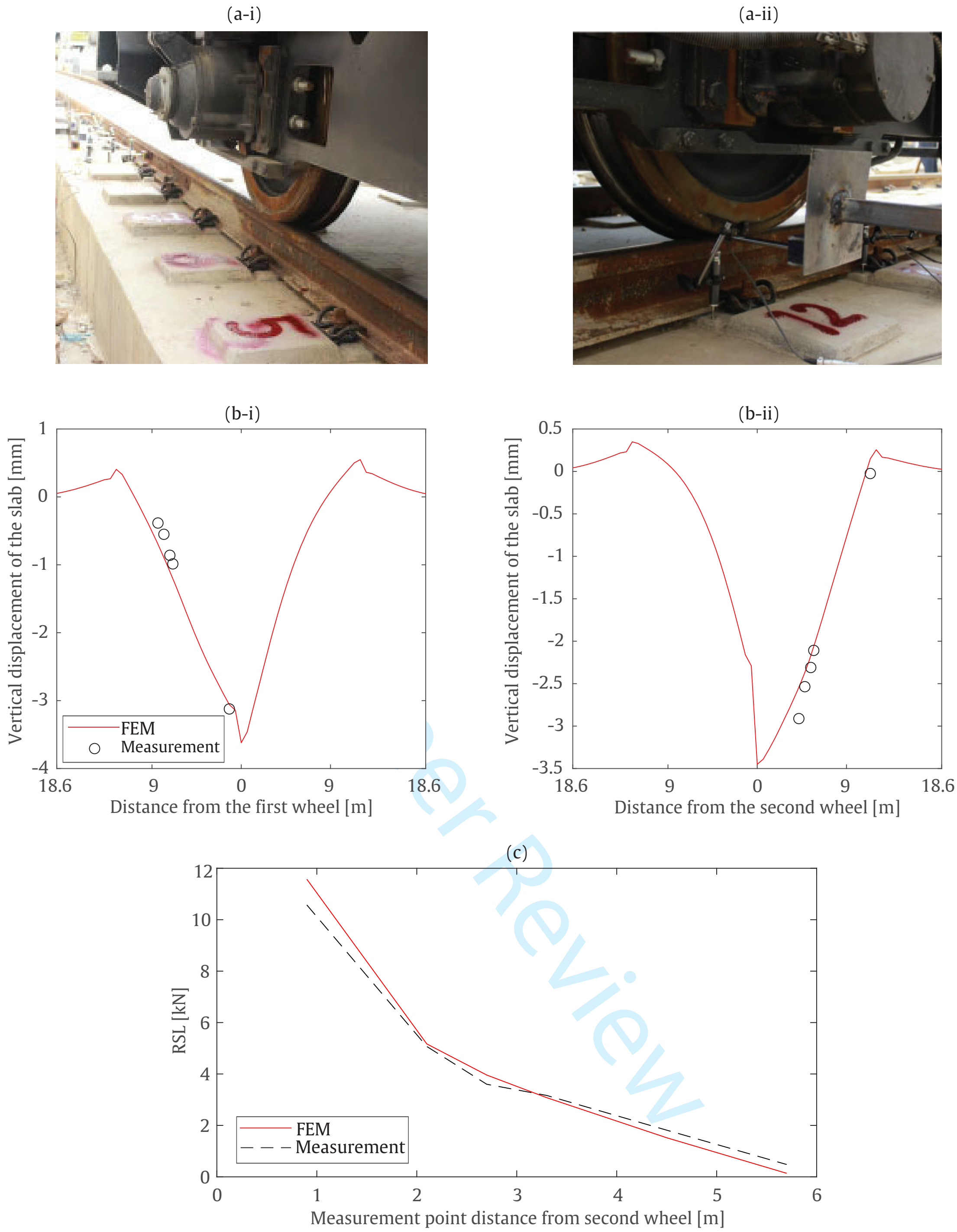

Figure 3. Model validation: first load case (a-i), second load case (a-ii), vertical displacement of the slab corresponding to the first load case (b-i), vertical displacement of the slab corresponding to the second load case (b-ii) and RSL value for various loading cases (c).

rail ($N.m^2$). This equation can be considered a generalized mathematical expression that can be used to improve the accuracy of the RSL ratio value in railway slab track designs. Since a wide range of variables was considered during the parametric study, and the most efficient ones were chosen to be used in Eq. 4, this equation can be considered an effective mathematical expression that can be utilized to design railway slab tracks.

Comparison of the current practices to the proposed mathematical expression

The majority of the prevailing researches are suitable for the ballasted track and they do not seem to be appropriate in the slab track systems. In this regard, it is still utilized the ballasted-based formulas for designing the slab track. The proposed mathematical expression was derived from an experimentally validated model, achieving a high regression value, thereby confirming the expression's verification. In order to evaluate importance of considering

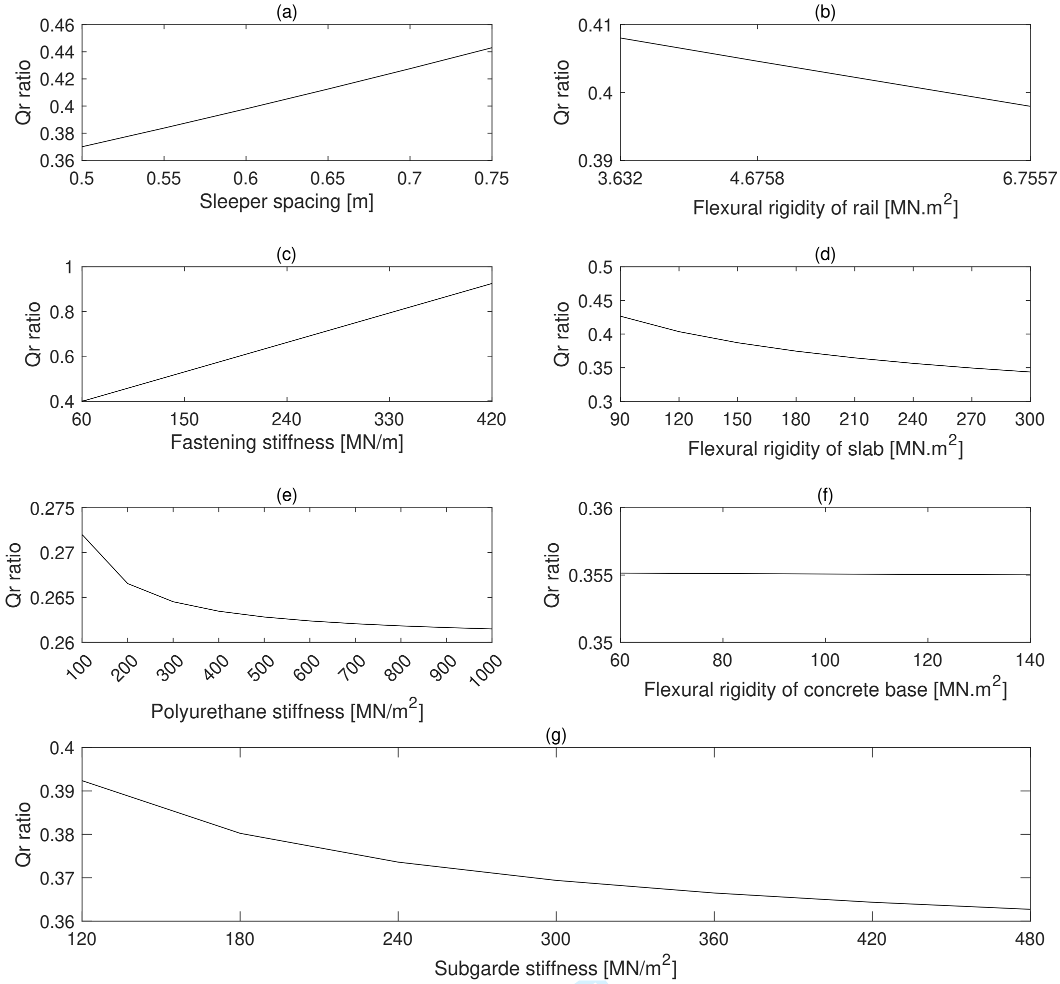

Figure 4. Effect of different parameters on RSL ratio: sleeper spacing (a), flexural rigidity of the rail (b), fastening stiffness (c), flexural rigidity of the concrete slab (d), polyurethane stiffness (e), flexural rigidity of the concrete base (f) and subgrade stiffness (g).

Table 3. Correlation matrix between dominant effective parameters on RSL and RSL ratio

Variable	Correlation			
	Rigidity of rail	Sleeper spacing	Fastening stiffness	Rail-seat load ratio
Rigidity of rail	1	0	0	-0.091
Sleeper spacing	0	1	0	0.194
Fastening stiffness	0	0	1	0.867
Rail-seat load ratio	-0.091	0.194	0.867	1

slab track condition, comparisons were made between the RSL obtained from the expression and those of the previous studies and standards. Table 4 presents the existing formulas provided in previous studies, standards and code of practices to calculate the RSL in the ballasted railway track. In Table 4, P, k, D and $D.F$ stand for the static wheel load, track modulus, wheel diameter and axle load distribution factor, respectively. As shown in Fig. 5, two parameters are considered in the comparison of expressions; sleeper spacing and the flexural rigidity of the rail. Concerning the first comparison (sleeper spacing), the initial values assigned to flexural rigidity of rail and track modulus are 6.7557 $\mathrm{MN.m^2}$ (UIC60) and 60 $\mathrm{MN/m^2}$, respectively. For the second comparison (flexural rigidity of the rail), the initial value assigned to sleeper spacing is 0.6 m. Also, it is important to mention that the Kerr expression accounts for $V = 0$. As depicted in Fig. 5a, significant differences between the AREMA and Australian Standards and the proposed mathematical expression are demonstrated, with sleeper spacing, increased from 24.3% to 38.2%. Conversely, better alignment with the proposed expression is exhibited by Kerr's expression, particularly within the normal range

Table 4. Existing expressions for RSL.

Model	Expression for RSL (metric)
AREMA[26]	$Q_r = P\frac{61.52L_s+12.811}{100}$
Kerr[36]	$Q_r = \frac{(1+0.33\frac{V}{D})P.L_s}{2}\sqrt[4]{\frac{k}{4EI}}$
Australian standard[27]	$Q_r = P\frac{D.F.}{100}$

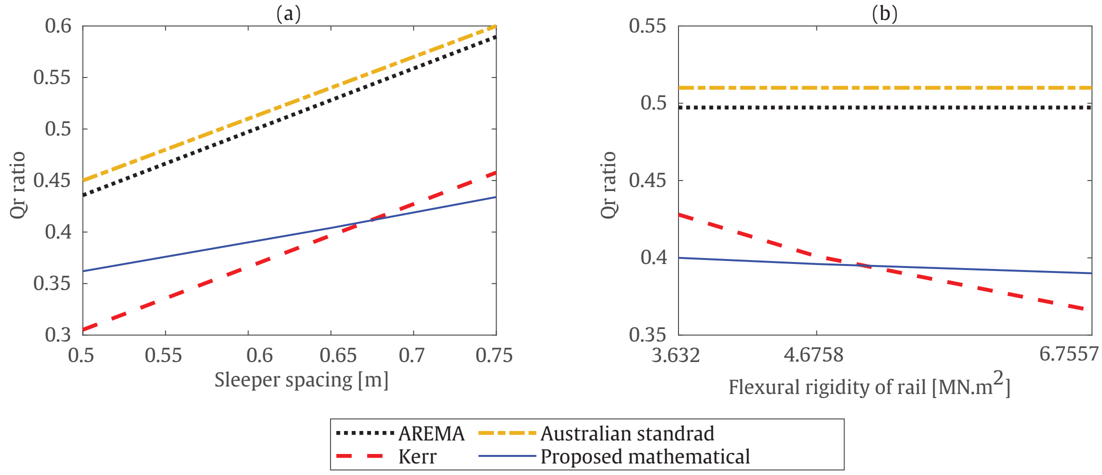

Figure 5. Comparison of the RSL ratio obtained from the mathematical expression and the ones proposed in the previous studies and current standards in terms of sleeper spacing (a) and flexural rigidity of the rail (b).

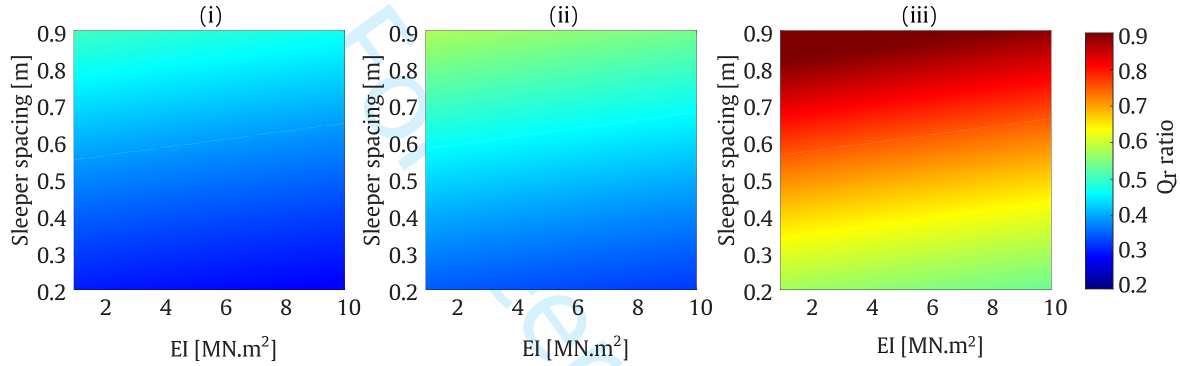

Figure 6. The RSL ratio versus sleeper spacing and flexural rigidity of rail, taking into account the influencing parameters considered in the mathematical expressions for soft (i), stiff (ii), and very stiff (iii) fastening systems.

of sleeper spacing (i.e., from 0.6 m to 0.7 m), where the difference is approximately 5.5%. In Fig. 5b, differences of around 31% between the AREMA and Australian Standards and the proposed expression are illustrated. A difference of approximately 7% from the suggested expression is shown by Kerr's expression.

Ultimately, these comparisons suggest that the existing expressions for calculating the RSL ratio for slab concrete may not be entirely suitable, as they are based on ballasted railway tracks. The only appropriate results are achieved for slab tracks with sleeper spacing greater than 0.65 m and specific rail profiles (i.e., UIC60) through the Kerr expression.

As mentioned earlier, the dominant parameters affecting the RSL ratio are sleeper spacing, the flexural rigidity of the rail, and the stiffness of the fastening system. Accordingly, Fig. 6 demonstrates the assessment of the RSL ratio while considering these parameters simultaneously. The considered values for different fastening systems were 60 MN/m, 100 MN/m, and 300 MN/m, corresponding to soft, stiff, and very stiff railway fastening systems. As depicted in Fig. 6, for the soft fastening system, the RSL ratio reaches up to 0.5, while this value increases to 0.6 and 0.9 for the stiff and very stiff fastening systems, respectively. Additionally, as indicated in Eq. (4), the highest RSL ratio is obtained with larger sleeper spacing and lower flexural rigidity of the rail.

Conclusion

In this paper, a 2D Finite Element (FE) model was developed in the FORTRAN environment and validated with experimental tests to evaluate the Rail Seat Load (RSL) in ballastless tracks. Based on the model, a parametric study was conducted to identify the dominant variables affecting the RSL ratio. Subsequently, a generalized mathematical expression was proposed to determine the RSL ratio for concrete slab tracks. The specific findings of the proposed investigation are outlined below:

- The FE model demonstrates good agreement with the experimental data when comparing vertical displacement and RSL value, thereby confirming the validity of the model.

- The dominant parameters affecting the RSL ratio are sleeper spacing, the flexural rigidity of the rail, and the stiffness of the fastening system. Following that, the RSL ratio has a direct relationship with sleeper spacing and fastening stiffness, whereas it has an inverse relationship with the flexural rigidity of the rail. In other words, increasing the sleeper spacing and fastening stiffness results in a higher RSL ratio, while increasing the flexural rigidity of the rail results in a lower RSL ratio.

- Within the considered range of variation of parameters, the RSL is nearly independent of the flexural rigidity of the slab and concrete base, polyurethane, and subgrade stiffness.

- The RSL ratio comparison for designing railway slab tracks among the AREMA, Australian standards, Kerr method and the proposed mathematical expression was demonstrated, showing that the current expressions, which were based on ballasted track data, are not sufficiently suitable for calculating the RSL in ballastless railway tracks. In more detail, the difference between the AREMA and Australian standards with the proposed formula was 32.8% and 31% by changing the sleeper spacing values and the flexural rigidity of the rail, respectively.

In conclusion, the proposed mathematical expression proves to be an effective for predicting RSL in railway slab tracks, a crucial parameter in the design of concrete railway slabs.

Declaration of Conflicting Interests

The author(s) declared no potential conflicts of interest with respect to the research, authorship, and/or publication of this article.

References

1. Matias SR and Ferreira PA. Railway slab track systems: review and research potentials, 2020. DOI:10.1080/15732479.2020.1719167.
2. Gautier PE. Slab track: Review of existing systems and optimization potentials including very high speed. *Construction and Building Materials* 2015; 92: 9–15. DOI: 10.1016/j.conbuildmat.2015.03.102.
3. Esveld C. Recent developments in slab track application. *Rail Tech Europe* 1999; .
4. Gailiene I and Laurinavičius A. The need and benefit of slab track: Case of lithuania, 2017. DOI:10.14256/JCE.1776.2016.
5. Remennikov AM and Kaewunruen S. Experimental load rating of aged railway concrete sleepers. *Engineering Structures* 2014; 76: 147–162. DOI:10.1016/j.engstruct.2014.06.032.
6. Sadeghi JM. Experimental evaluation of accuracy of current practices in analysis and design of railway track sleepers. *Canadian Journal of Civil Engineering* 2008; 35(9): 881–893. DOI:10.1139/L08-026.
7. Sadeghi J and Barati P. Comparisons of the mechanical properties of timber, steel and concrete sleepers. *Structure and Infrastructure Engineering* 2012; 8(12): 1151–1159. DOI: 10.1080/15732479.2010.507706.
8. Romero MJG, Edwards JR, Barkan CP et al. Advancements in Fastening System Design for North American Concrete Crossties in Heavy-haul Service. In *Proceedings of the AREMA 2010 Annual Conference & Exposition*. 618, pp. 1–24.
9. Wei S, Ave NM, Edwards JR et al. Gauging of Concrete Crossties To Investigate Load Path in. In *Proceedings of the 2014 Joint Rail Conference JRC2014*. ISBN 9780791845356, pp. 1–7. DOI:10.1115/JRC2014-3840.
10. Mishra D, Tutumluer E, Boler H et al. Railroad Track Transitions with Multidepth Deflectometers and Strain Gauges. *Transportation Research Record* 2014; 2448: 105–114. DOI: 10.3141/2448-13.
11. Wheeler LN, Andy Take W, Hoult NA et al. Use of fiber optic sensing to measure distributed rail strains and determine rail seat forces under a moving train. *Canadian Geotechnical Journal* 2019; 56(1): 1–13. DOI:10.1139/cgj-2017-0163.
12. Grasse JS, Wei S, Edwards JR et al. Field study of load path in rail and concrete crosstie system. *Electronic Journal of Structural Engineering* 2014; 14: 29–38.
13. Manda KR. Vertical Load Path Under Static and Dynamic Loads in Concrete Crosstie and fastening systems. In *Proceedings of the 2014 Joint Rail Conference JRC2014*. ISBN 9780791845356. DOI:10.1115/JRC2014-3832.
14. Askarinejad H, Dhanasekar M, Boyd P et al. Field Measurement of Wheel-Rail Impact Force at Insulated Rail Joint. *Experimental Techniques* 2015; 39(5): 61–69. DOI: 10.1111/j.1747-1567.2012.00867.x.
15. Gao Z, Qian Y, Dersch MS et al. Compressive stress distribution in prestressed concrete and its effect on railroad crosstie design. *Construction and Building Materials* 2017; 151: 147–157. DOI:10.1016/j.conbuildmat.2017.05.186.
16. Greve M, Dersch MS, Edwards JR et al. Analysis of the Relationship Between Rail Seat Load Distribution and Rail Seat Deterioration in Concrete Crossties. p. V001T01A016. DOI:10.1115/JRC2014-3775.
17. Greve MJ, Dersch MS, Edwards JR et al. Examination of the Effect of Concrete Crosstie Rail Seat Deterioration on Rail Seat Load Distribution. *Transportation Research Record: Journal of the Transportation Research Board* 2015; 2476: 1–7. DOI: 10.3141/2476-01.
18. Zhang X, Zhao C, Ren X et al. Experimental investigation on the characteristics of the dynamic rail pad force and its stress distribution in the time and frequency domain. *Proceedings of the Institution of Mechanical Engineers, Part F: Journal of Rail and Rapid Transit* 2020; 234(2): 201–213. DOI: 10.1177/0954409719838116.
19. Van Dyk BJ, Scheppe AJ, Edwards JR et al. Methods for quantifying rail seat loads and a review of previous experimentation. In *Proceedings of the Institution of Mechanical Engineers, Part F: Journal of Rail and Rapid Transit*, volume 230. pp. 935–945. DOI:10.1177/0954409715569862.
20. Momoya Y, Ito K and Kikkawa S. Settlement of ballasted track with large sleeper spacing. In Tutumluer E, Nazarian S, Al-Qadi I et al. (eds.) *Advances in Transportation Geotechnics IV*. Cham: Springer International Publishing. ISBN 978-3-030-77234-5, pp. 77–86.
21. Lojda V, Van Belkom A and Krejčiříková H. Investigation of the Elastic Modulus of Polymer Sleepers under a Quasistatic and Cyclic Loading. *Civil and Environmental Engineering* 2019; 15(2): 125–133. DOI:10.2478/cee-2019-0016.
22. Shi C, Zhao C, Yang Y et al. Macro-meso dynamic analysis of railway transition zone: Hybrid DEM/FDM simulation and experimental validation. *Soil Dynamics and Earthquake Engineering* 2020; 135(May): 106191. DOI:10.1016/j.soildyn.2020.106191.
23. Trizotto M, Dersch MS, Edwards JR et al. Analytical elastic modeling of rail and fastener longitudinal response. *Transportation Research Record* 2021; 2675(5): 164–177. DOI:10.1177/0361198120985848.
24. UITP. Urban Rail Transport. Technical report, Deliverable D0602 . Final Consolidated Report, 2010.

25. Sadeghi J, Liravi H and Esmaeili MH. Experimental investigation on loading pattern of railway concrete slabs. *Construction and Building Materials* 2017; 153: 481–495. DOI:10.1016/j.conbuildmat.2017.07.025.
26. AREMA, American Railway Engineering and Maintenance-of-Way Association. Technical report, AREMA, Landover, Maryland, 2012.
27. Australian Standard. Pre-stressed concrete sleepers in Railway track materials. Technical report, 2002.
28. Zhang TW, Cui YJ, Lamas-Lopez F et al. Modelling stress distribution in substructure of French conventional railway tracks. *Construction and Building Materials* 2016; 116: 326–334. DOI:10.1016/j.conbuildmat.2016.04.137.
29. Sadeghi J, Khajehdezfuly A, Esmaeili M et al. Investigation of rail irregularity effects on wheel/rail dynamic force in slab track: Comparison of two and three dimensional models. *Journal of Sound and Vibration* 2016; 374: 228–244. DOI: 10.1016/j.jsv.2016.03.033.
30. Przemieniecki J. *Theory of Matrix Structural Analysis*. New York, 1985. ISBN 0521855705. DOI:10.1017/cbo9780511546112.
31. Sadeghi J, Khajehdezfuly A, Esmaeili M et al. An Efficient Algorithm for Nonlinear Analysis of Vehicle/Track Interaction Problems. *International Journal of Structural Stability and Dynamics* 2015; 16(08): 1550040. DOI:10.1142/s0219455415500406.
32. Sadeghi J, Seyedkazemi M and Khajehdezfuly A. Nonlinear simulation of vertical behavior of railway fastening system. *Engineering Structures* 2020; 209: 110340. DOI:https://doi.org/10.1016/j.engstruct.2020.110340.
33. Pucinotti R. Reinforced concrete structure: Non destructive in situ strength assessment of concrete. *Construction and Building Materials* 2015; 75: 331–341. DOI:10.1016/j.conbuildmat.2014.11.023.
34. Zhu W, Gibbs JC and Bartos PJ. Uniformity of in situ properties of self-compacting concrete in full-scale structural elements. *Cement and Concrete Composites* 2001; 23(1): 57–64. DOI:10.1016/S0958-9465(00)00053-6.
35. Adamowski J, Fung Chan H, Prasher SO et al. Comparison of multiple linear and nonlinear regression, autoregressive integrated moving average, artificial neural network, and wavelet artificial neural network methods for urban water demand forecasting in Montreal, Canada. *Water Resources Research* 2012; 48(1): 1–14. DOI:10.1029/2010WR009945.
36. Eisenmann J. Stress distribution in the permanent way due to heavy axle loads and high speeds. *Proceedings of AREA* 1970; 71: 24–59.